

A statistical approach to estimates of geomorphological-morphotectonic diversity for evaluating the scientific value of geosites: a case study from the southeastern Lut desert, Iran

Pouya Sadeghi-Farshbaf^{1*}, Mohammad Mahdi Khatib¹, Naser Rezaei²

¹Department of Geology, University of Birjand, Birjand, Iran;
e-mails: pouya.sadeghi@birjand.ac.ir, mkhatib@birjand.ac.ir

²Department of Natural Heritage, Research Institute of Cultural Heritage & Tourism (RICHT), Tehran, Iran;
e-mail: n.rezaei@richt.ir

*corresponding author

Abstract

The present study aims to investigate the diversity index (dv-index) of morphotectonic and geomorphological landforms as one of the scientific value indices for evaluation of the geotouristic potential of the southeastern Lut desert using topographic statistical analysis. Scientific index scoring in most models is based on descriptive assessment by geotourists and experts. Statistical analysis of the dv-index in the present study helps experts to base their scoring on scientific methods. The dv-index is controlled by several items. In the present study, we analyse two of these, including the classification of topographic continuity pattern (TCP) and topographic slope position correlation (TSPC). For this purpose, a network of section lines is used to analyse slope continuity. The TSPC analysis is performed by using two parameters of absolute value and slope position. Results for these two evaluated items indicate a score of 1.46 (out of 2) for the dv-index. Given a rating of 5, the score obtained for the two items is a high one. Therefore, an initial estimate of the dv-index indicates a significant scientific value of the study area.

Key words: diversity index, geomorphosite, topography, statistical rating

1. Introduction

Geological heritage is a special term that refers to sites and areas with specific geological phenomena that have scientific, educational, cultural and aesthetic values. Over the last two decades, there has been a growing interest among the geosciences in topics related to geoheritage: geoconservation, geotourism and geoparks (Reynard & Brilha, 2017). One of the most important aspects of geotourism is nature-based tourism. According to some researchers, geotourism is defined as tourism in geologi-

cal-geomorphological landscapes, rock outcrops and fossil-bearing layers (Coratza & Giusti, 2005; Dowling & Newsome, 2006; Hadžić et al., 2010; Ne-manj, 2011). Today, however, the scope of geotourism has become very wide and encompasses highly sensitive scientific-educational topics and values. The academic concept of geotourism, which focuses on university research, was defined in 1995 as a new form of niche tourism (Hose, 2012). Geotourism is tourism that preserves or enhances the geographical identity of a site, and includes not only the environment, but also cultural heritage, aesthet-

ics of the site and, most importantly, the prosperity of local inhabitants (Pereira et al., 2008). While most references on geoheritage and geotourism are related to non-urban areas, there is also geoheritage within the urban areas and thus it is possible to do urban geotourism (Rodrigues et al., 2011; Pica et al., 2016; Kubalíková et al., 2017; Reynard et al., 2017; Melelli, 2019). However, various aspects of tourism, including rural tourism (Oliver & Jenkins, 2003; Farsani et al., 2013; Stoffelen & Vanneste, 2015), health geotourism (Rocha & da Silva, 2014), climate tourism (Scheyvens, 1999; Buckley, 2003; Horváth & Csüllög, 2012) and cultural-social tourism (Hurtado et al., 2014; Jana et al., 2016) have some aspects that allow us to consider these activities as geotourism. Geomorphosites are “geomorphological landforms that have acquired a scientific, cultural/historical aesthetic and/or social/economic value due to human perception or exploitation” (Panizza, 2001; Reynard & Panizza, 2005). Attractive geomorphological-geological sites are defined as geomorphosites (Panizza, 2001). However, a combination of geomorphosites with cultural elements increases their value (Comanescu et al., 2012). Sustainable development in geotourism is one of the most important factors in regional economic and cultural prosperity. Therefore, identifying and introducing high-value geosites is of key importance in the regional tourism boom. Connecting landscape, cultural heritage and sports facilities with unique geological and geomorphological features, encourages both local and regional sustainable development (Burlando et al., 2011). Geosites are sites of scientific interest based on geology or geomorphology that can serve various purposes such as research, conservation, education, tourism and sustainable development (Suzuki & Takagi, 2018). Geomorphosites are defined as areas with specific geomorphological processes that are important for our understanding of the evolution of the earth, and therefore geomorphosites can have both scientific value and added value (Reynard & Panizza, 2005). The growing importance of geomorphosites among scientists and the general public alike leads to increasing scientific experience, highlighting the natural-cultural heritage, expanding communication with neighbouring geosites, and contributing to regional economic and social development.

The abundance of historical sites and geological phenomena in Iran has made it one of the countries with a high potential for tourism and geotourism purposes. From a geological point of view, various studies have described potential global geosites in different regions of Iran including geotourism potential in Kashmar (Taherpour, 2012), geologi-

cal features for geotourism in the Sahand Volcano (Mehdipour Ghazi, 2013), geological heritage in the Zagros fold-thrust belt (Habibi et al., 2017), morphometric characteristics in the Lut desert (Ghodsi, 2017) and geomorphosite assessment in the Qeshm Geopark (Hosseinzadeh et al., 2018). However, in the case of topographic and morphotectonic studies, the Lut desert can be a good choice in view of a lack of vegetation and a complex tectonic history.

Despite the descriptive studies mentioned above, the lack of a scientific scoring and ranking system in Iran is very noticeable. It would be fascinating for geotourists and scientists to know how close a scientific index of a geological feature in one geosite is to their scientific-educational goals. In addition, if similar studies are done for other regions, a scientist or visitor interested in geomorphosites of scientific value can easily decide which site to choose and visit. For example, if one site is rated 1.5 and the other 1.6, and the cost of visiting the second site is high, the first site will definitely be a good alternative to visit. Several attempts have been made to assess geodiversity (Forte et al., 2018; Zwoliński et al., 2018) and geomorphodiversity (Melelli et al., 2017; Ferrer-Valero, 2018) with a quantitative approach. Scientific scoring in different models has different ranges of scores. Expert scoring of the *dv*-index ranges from 0 to 5 in the Hadžić model (Hadžić et al., 2010), for instance. Another example is the methodology prepared by the Paleontological Museum of Elche (MUPE) for the Fossils and Heritage Project of Alicante (FO-PALI) for scientific assessment that is based on ten criteria or parameters: abundance of similar outcrops, key locality, palaeodiversity-geodiversity, palaeodisparity, conservation status of immovable and movable property, taphonomic-genetic interest, geological interest (including biostratigraphy, lithostratigraphy, tectonics and geomorphology), utility to illustrate processes and scientific potential) equally weighted and ranked from 0 to 4 (Corbí et al., 2018). Although scientific scoring in most studies is based on descriptive words or numbers equivalent to descriptions, the main purpose of the present study is to standardise scoring based on statistical principles. For example, Mikhailenko & Ruban (2019) described geotourism attractions in terms of physical visibility, interpretation (clarity) and aesthetic attractiveness, while there is no standard criterion for measuring this attraction. In other words, there are two approaches to investigate the *dv*-index of morphotectonic and geomorphological landforms: one is evaluation of a landform based on its apparent characteristics (which may be emotional and arbitrary) and there is no specific criterion

from the evaluator's point of view, and the other is evaluation based on a set of calculable criteria in the form of a method that can converge decision-making processes while preserving the value of personal approaches. The statistical algorithm presented here integrates descriptive approaches and guides them into a specific evaluation path. Since the numerical results defined in a given range provide a better understanding of a high or low value, the outputs of the evaluation of the present study are in the form of scoring. The scores for the two studied scientific indices (out of other dv-index items) are calculated separately in a range of 0 to 2.

2. Geographical and geological setting

As part of the Alpine-Himalayan orogenic belt that is subjected to continental convergence, the Iranian plateau is the origin of various tectonic phenomena related to the transpressional system. Massive folds and faults, along with diverse and complex morphotectonic structures, are all related to this system. Strong folding and thrusting during Alpine orogeny proper in the Late Cretaceous-Cenozoic affected most of Iran, with the exception of the rigid Lut block in the eastern part of the country (Stocklin, 1968). The Iranian arid areas and deserts, particularly the Lut desert, have many geomorphological

and geological features (Maghsoudi & Emadoldin, 2007). The northward motion of central Iran - Lut, relative to Eurasia along N-S strike-slip fault systems (Farbod et al., 2011), make the margins of the Lut block an appropriate platform for the development of morphotectonic phenomena.

The Lut (Dasht-e Lut) is located in southeastern Iran and encompasses an area of more than 50,000 square kilometres between parts of the provinces of Kerman, Sistan and Baluchestan and South Khorasan. The approximate length and width of this desert, which stretches from the northwest to the southeast, are 320 km and 160 km, respectively. The Lut desert and its environmental system, as one of the unique deserts of the world in terms of outstanding features, have lots of potential and outstanding universal values, including the highest and longest yardangs (kaluts) and very high sand dunes and nebkhas (Maghsoudi et al., 2017). The yardangs and corridors in the Lut desert are aligned NNW-SSE parallel to the prevailing direction of the strong local 120-days-wind and cover about 31 and 42 per cent of the western part of the Lut desert, respectively (Ehsani & Quiel, 2008).

Tectonic deformations along the strike-slip faults in eastern Iran are controlled by the collision of the Eurasian/Arabian plates. This convergence of plates, which began in the Eo-/Oligocene (e.g., Agard et al., 2005; Vincent et al., 2005), caused

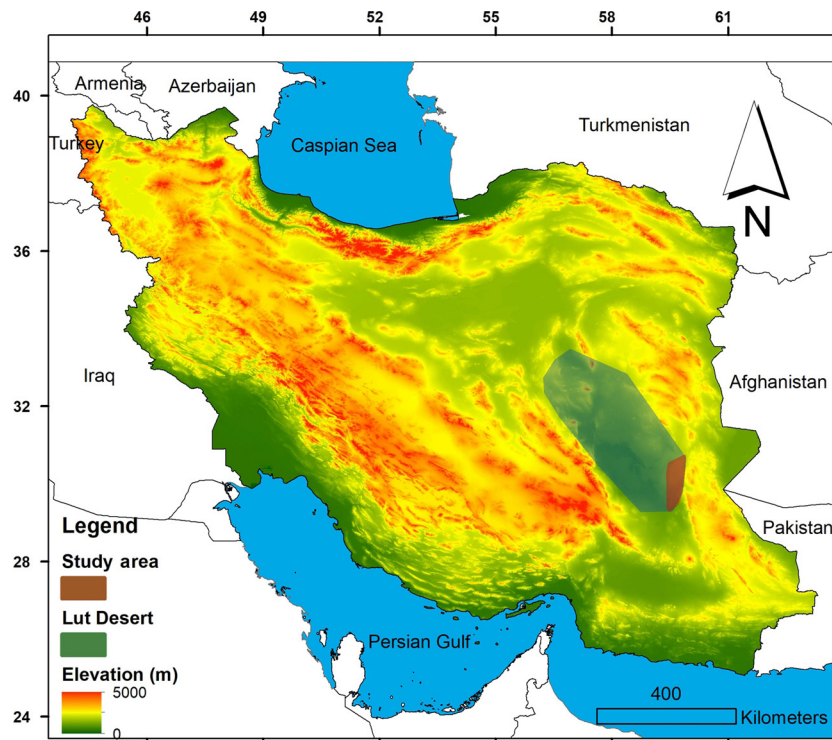


Fig. 1. Location of the study area in the Lut desert on the digital elevation model (DEM) map of Iran

widespread deformations across Iran, especially the margins of the Lut Block. South of 34°N, right-lateral shear is accommodated on a series of parallel N–S right-lateral faults running along the eastern margin (the Sistan Suture Zone fault systems) and the western margin (the Nayband–Gowk–Sabzevaran fault system) of the Dasht-e Lut (Walker et al., 2009). Tectonically, the Lut desert is bounded in the east by the N–S striking Nehbandan fault and in the west by the N–S striking Nayband fault. The Nehbandan fault in the southern part trends to the east, and the Nayband fault plays an important role in the formation of the Tabas Sedimentary Basin and the Shotori Mountains. Both faults have a right-lateral strike-slip mechanism. The study area is located in the southeast of the Lut desert (Fig. 1). This range is bounded in the east by the Kahurak and Western Neh faults, and mainly consists of sand dunes (Fig. 2). Single or complex sand dunes begin in the

form of a crescent (Barkhan) or are stretched at an elevation of 1,100 m along the eastern margin of the Lut desert and gradually extend near the central Lut Hole to a height of 250 metres. Given the north-west-southeast carving direction of the Kaluts, it seems that wind direction in moving these sands is quite southerly and the catchment area is confined to the eastern margin of the Lut desert. The yardangs size and height in the centre and north of the region exceed the southern side that represents a further evolution of yardangs which exist in the south side of the region (Ghodsi, 2017). Therefore, given the further evolution of the yardangs and kaluts from the north to the south of the Lut, these features can be said to be more stable in the southern Lut desert, and therefore morphotectonic studies in that area are more reliable. In addition to erosional features, most of the landforms in the Lut desert are controlled by strike-slip faults, as noted for Lut tectonics. Even the drainage basins are affected by tectonics in the area. For instance, Moghimi (2009) showed that the sinuosity of rivers in the Lut basins is due to a morphotectonic effect, and the territory of important Lut unit drainage basins is limited to tectonic lines and forms the bounds of basins. Therefore, the sum of all these landforms and terrain features within the study area generates the same topography that is statistically analysed in the present research according to the following sections for scoring.

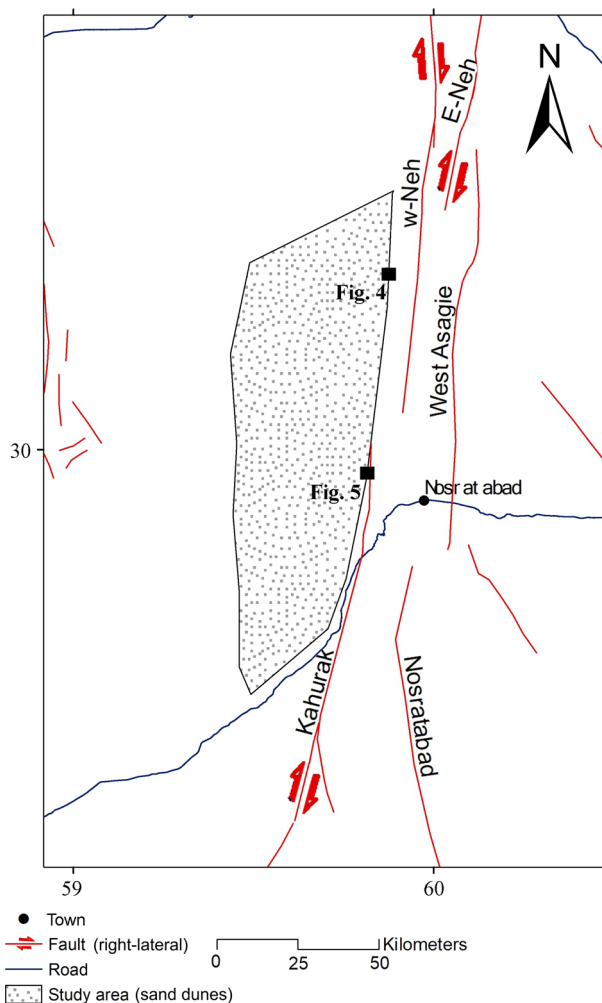


Fig. 2. Schematic outline representing faults around the study area and the main access road. Solid black squares show locations of Figures 4 (morphotectonic feature) and 5 (fault boundary of sand dunes)

3. Material and methods

Both TCP and TSPC classifications have been investigated for preliminary estimates of the dv -index. The TCP item directly reflects the tectonic effects of the area because topographic continuity occurs under passive tectonic conditions, namely weathering and erosion over tectonic activities. To date, a considerable number of studies have demonstrated these relationships. Tectonic control of alluvial architecture is commonplace in extensional, transcurrent and compressional tectonic terrains (Alexander & Leeder, 1987). Berberian (1995) showed how blind thrust faults controlled topographic and morphotectonic patterns in the Zagros fold and thrust belt. Drewes (1972) pointed out the topographic continuity and its relation to tectonic features. The TSPC item can be said to reflect the homogeneity of the TCP in all directions over a range whose calculation ultimately results in recognition of the types of topography within a single geomorphosite. For educational purposes such as morphotectonic and morphological typology, the ability to access a

collection of valuable landforms in the form of geomorphosites, considering the extent, and location of an area for the scientific-educational visit is very important. Statistically, the desirability of these two items increases the possibility of better access to the whole site on the one hand and estimation of scientific professional goals on the other.

The mathematical definition of different levels of continuity has been used to evaluate the TCP item. The three main types of continuity are step-wise (SC), quick change (QC) and continuous rate of change (CRC) (Fig. 3). If we wish to define these three classes in geology, we consider SC as vertical topographic reliefs, QC as active tectonics and CRC as passive tectonics. Therefore, fault scarps as well as deep river channels exhibit an SC pattern in their topography, whereas active tectonic effects (higher uplift or subsidence rates than local erosion) and the placement of indurated formations along loose ones show the QC pattern. A high percentage of QC

reflects the important role of structural controllers such as faulting and folding in the current topographic pattern. When the erosion rate exceeds the rate of tectonic movements, the dominant topography as smooth reliefs follows the CRC pattern.

Analysing different TCPs along multiple sections can reveal the tectonic or weathering control of the topography. For example, in scientific-educational studies, Figure 3 shows the rough to the smooth topography from active tectonics to passive tectonics. Therefore, the different extent of these topographic surfaces in a geomorphosite controls the dv-index. Figures 4 and 5, for example, illustrate tectonic and tectonic/aeolian control of topographic variations, respectively. As can be seen in Figure 4, topography follows the QC pattern with different resistivity layers. In addition, normal faulting causes localised drag and rotation of adjacent layers close to the fault plain. This makes it impossible to remove the topography from the QC pattern even

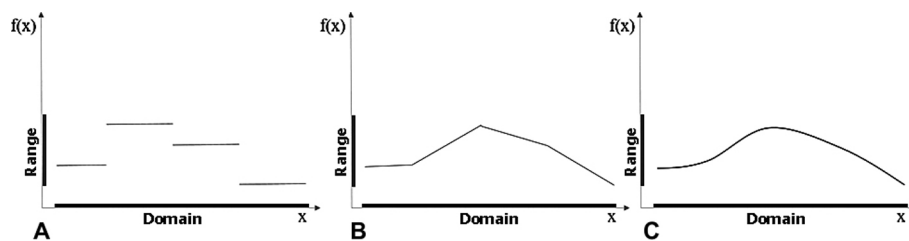


Fig. 3. Different functions of continuity, including: A – step-wise; B – quick change; C – continues rate of change. The x and f(x) axes represent the domain and range of the function, respectively

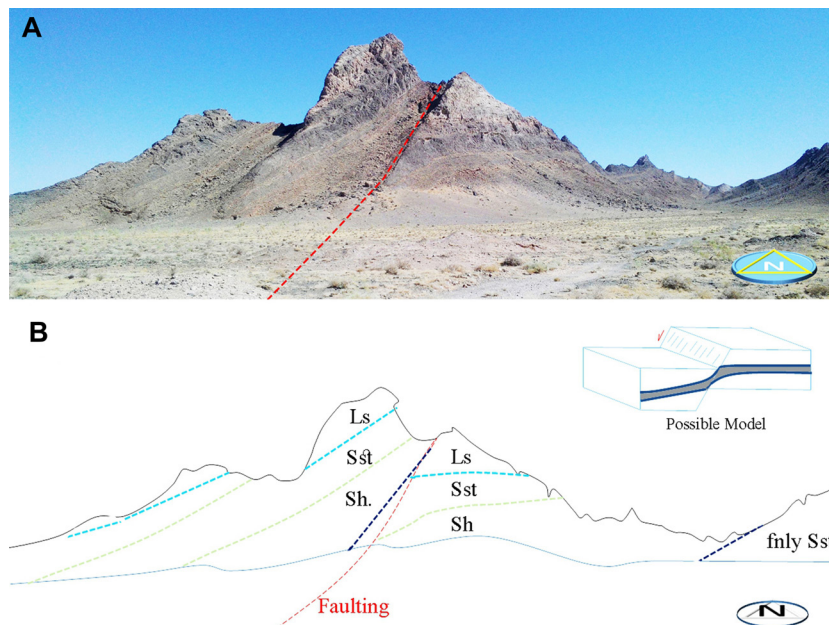


Fig. 4. Tectonic control of topographic variations. A – morphotectonic structure at position indicated in Figure 2: B – Sketch of (A) showing the dragged and rotated sedimentary sequences by normal faulting (red dashed line). Ls = limestone; Sst = sandstone; Sh = shale; fnly Sst = fine sandstone



Fig. 5. The eastern boundary of the study area, including dune and morphotectonic sites restricted by the Kahurak fault (red dashed line) at position indicated in Figure 2. This region represents tectonic/aeolian control of topographic variations

as it continues to erode and reach the bottom layers. Figure 5 shows both QC and CRC patterns side by side. Here, the QC pattern is related to the morphotectonic site, indicating the tectonic controller (faulting) and the CRC pattern is linked to the dune site, indicating the aeolian controller.

The TSPC analysis is performed using two parameters of absolute value and slope position. The absolute value is defined as follows (Vico & Porporato, 2009):

$$S = \sqrt{(\partial_x h)^2 + (\partial_y h)^2}, \quad (1)$$

where S is the height of a topographic field $h(x,y)$. Therefore, with the elevation field, it becomes possible to express a quantitative and absolute local slope value.

In the next step, the slope position is obtained by using the following trigonometric inverse function [9]:

$$a = \tan^{-1} \frac{(\partial_y h)}{(\partial_x h)}. \quad (2)$$

It should be noted that if the x and y axes correspond to the reference meridian, then a is measured counterclockwise from the west, and S is defined as the degree of height change per horizontal unit length. This measurement can easily be expressed in degrees according to the horizontal plane:

$$\beta = \tan^{-1} S. \quad (3)$$

Finally, it is assumed that such an elevation field is realistically explained by the sum of a homogeneous random field of zero mean $z(x,y)$ and

an independent deterministic linear trend (Vico & Porporato, 2009):

$$h(x,y) = z(x,y) + b_0 + b_x x + b_y y. \quad (4)$$

A linear trend is generally adequate for the description of weak trends and can be interpreted as a local linear approximation of more complex inhomogeneities (Vico & Porporato, 2009).

The scoring system in the present study is based on z-scoring, converting z-values to t-values, and normalising final scores. z-value means the distance of each datum from the average value of the numbers in a data set, expressed as standard deviation. Given the population mean and population standard deviation, the z-score of a sample value x (Kreyszig, 1979) can be calculated as follows:

$$z_{sc} = \frac{x - \mu}{\sigma}, \quad (5)$$

where μ is the mean of the population, and σ is the standard deviation. In the present study, x was replaced by frequency and correlation percentages in TCP and TSPC analyses, respectively. In addition, since the use of the z-scores is not possible here because the z-scores are negative when the sample values are lower than the mean of the population, the z-values have been converted to t-values that have a mean of 50 and a standard deviation of 10 (Wimberley, 1975; Adeyemi, 2011; Salvia et al., 2012; Neukrug & Fawcett, 2014), as follows:

$$T_{sc} = 10Z + 50 \quad (6)$$

The scientific score has therefore been calculated with a simple proportion as follows:

$$Sci_{sc} = (ST_{sc} - Stdev_p)Max_{sc} / ST_{scsS'} \quad (7)$$

where ST_{sc} is the sum of t-scores, $Stdev_p$ is a standard deviation for the entire population, and Max_{sc} is the maximum score in an arbitrary range that equals 1 in the present study. Since our scores for each item range from 0 to 1 and the Sci_{sc} is not zero, the calculated Sci_{sc} should eventually be normalised to a range of 0 to 1. For this purpose, the Max and Min of the Sci_{sc} must be calculated. Therefore, it is first necessary to digitise the data once in the best and once in the worst sample distribution. By obtaining the range of Sci_{sc} changes, the scores have been normalised (Patro & Sahu, 2015) to the desired range of 0 to 1 as follows:

$$NSci_{sc} = (Sci_{sc} - Sci_{sc.min}) / (Sci_{sc.max} - Sci_{sc.min}), \quad (8)$$

where $NSci_{sc}$ is normalised Sci_{sc} , and $Sci_{sc.max}$ and $Sci_{sc.min}$ are the upper and lower scoring ranges, respectively.

4. Results and discussion

The nine parallel and transverse sections have been selected as hypothetical topographic hiking trails. All sections start at low altitudes. Topographic variations in each section have been examined by TCP analysis. Each section consists of several red and green segments (Fig. 6). Unlike the red segments, the green ones are parts of the Topographic Profile Line (TPL) that are visible from the starting point of hiking.

Outputs of the elevation graphs corresponding to seven transverse and two longitudinal sections covering the study area homogeneously have been used for TCP classification (Fig. 7). The straight dashed lines in each section in Figure 7 represent the overall slope of the hiking trail, and have therefore been considered as the Intermediate Topographic Profile Line (ITPL) in each section. The location of the first intersection of the TPL and ITPL in each section has been marked (solid blue circles). To minimise the computational error caused by local topographic roughness, in the sections with solid blue circles, the longest TPL from the one of the starting or ending points of the section leading to the blue circles has been selected for TCP analysis.

According to Figure 8, in the direction perpendicular to a fault strike, the overall geometry of the TPL is concave or a combination of concave and convex lines relative to the ITPL (e.g., sections 1 to 5 in Figure 7). The convexity of the TPL over the ITPL can be due to folding (e.g., Section 6 in Figure 7). In

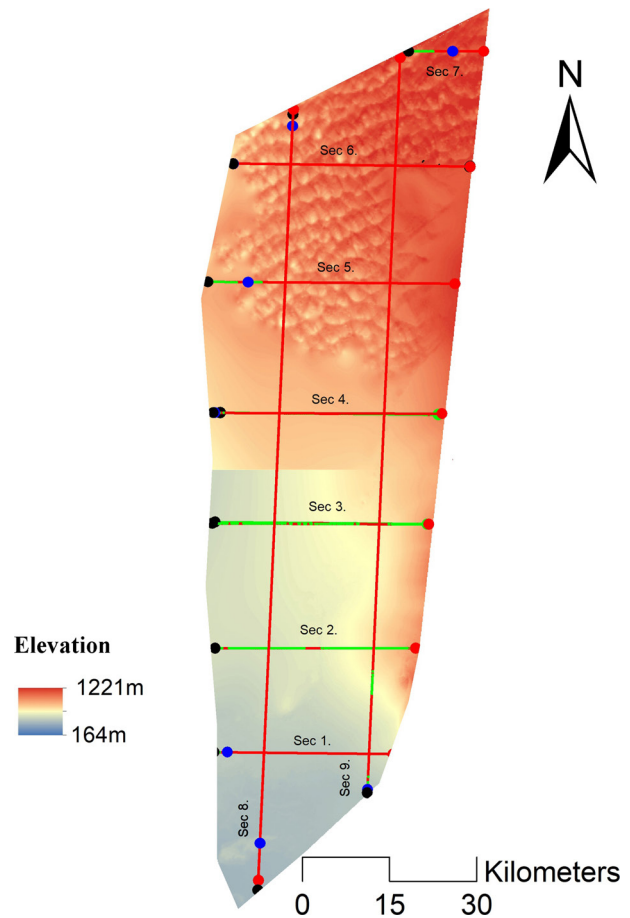


Fig. 6. A network of sections required for TCP analysis in the study area on the digital elevation model (DEM) map. The green and red segments are visible and hidden TPLs from the starting point of hiking, respectively. The solid black circles represent the starting point of hiking, and the blue solid circles the location of the first intersection of TPL and ITPL. The solid red circles also represent the ending point of the red segment

addition, the relative convergence of the TPL to the ITPL indicates hiking along the fault strike. Therefore, to validate the interpretation of transverse sections, it is necessary to have parallel sections along the fault strikes to cover all transverse sections. Parallel sections should show the highest level of convergence with the ITPL if the interpretation of tectonic control of the transverse sections is correct. Accordingly, sections 8 and 9, which cover all sections 1-7 (Fig. 7), with the highest level convergence with the ITPL compared to the other sections, confirm the tectonic control of sections 1 through 7 by structural elements including faulting and folding.

A comparison of the pattern of sections in Figure 7 with the reference sections in Figure 8, as well as considering the discussed topics of concavity, convexity and convergence of the TPLs to the ITPLs, represents SC, QC and CRC patterns with a

frequency of 20%, 50% and 30%, respectively. The high percentage of the QC pattern is due to the presence of structural controllers of the topography at the eastern boundary of the study area, the Kahurak and West Neh faults, and shows the value of

morphotectonic studies for the study area, in spite of the predominance of the steepness of the elevation points (Fig. 9).

Figure 9 separates the boundaries of the four topographic regions by the frequency of elevation

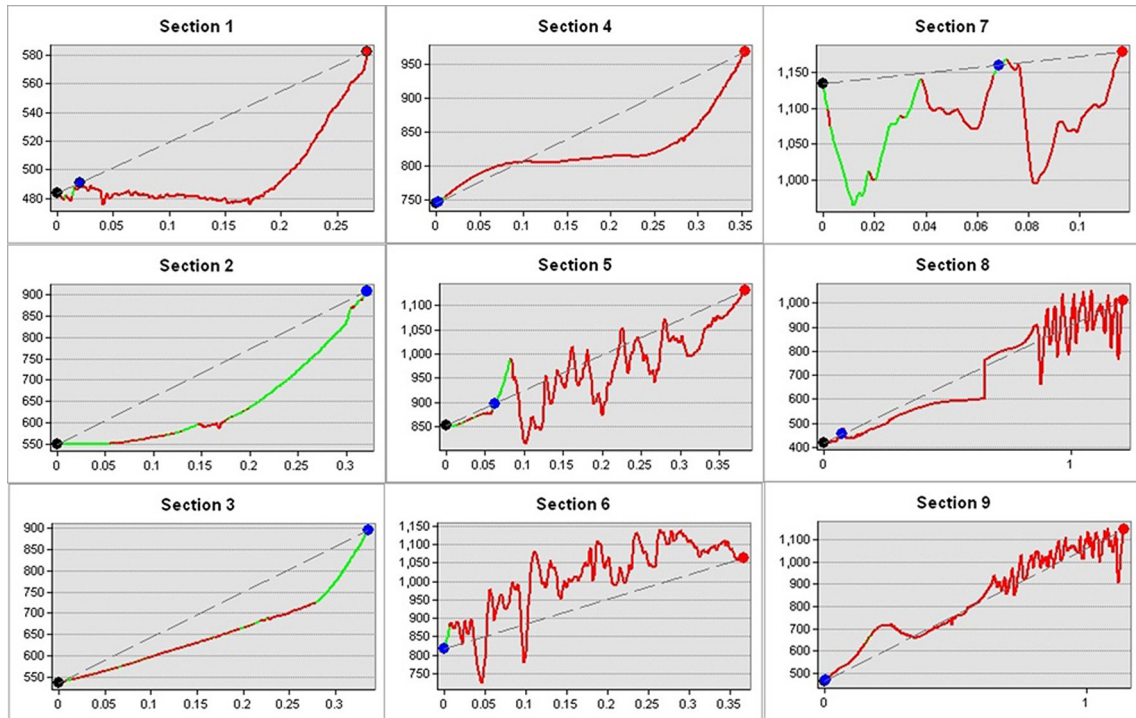


Fig. 7. Comparison of seven sections shown in Figure 6. Vertical and horizontal axes represent altitude (m) and distance (km), respectively. The straight dashed lines show the ITPLs from the beginning to the end of hiking. The green and red segments are visible and hidden TPLs from the starting point of hiking, respectively. The solid black circles represent the starting point of hiking, and the blue solid circles represent the location of the first intersection of TPL and ITPL. The solid red circles also represent the ending point of the red segment

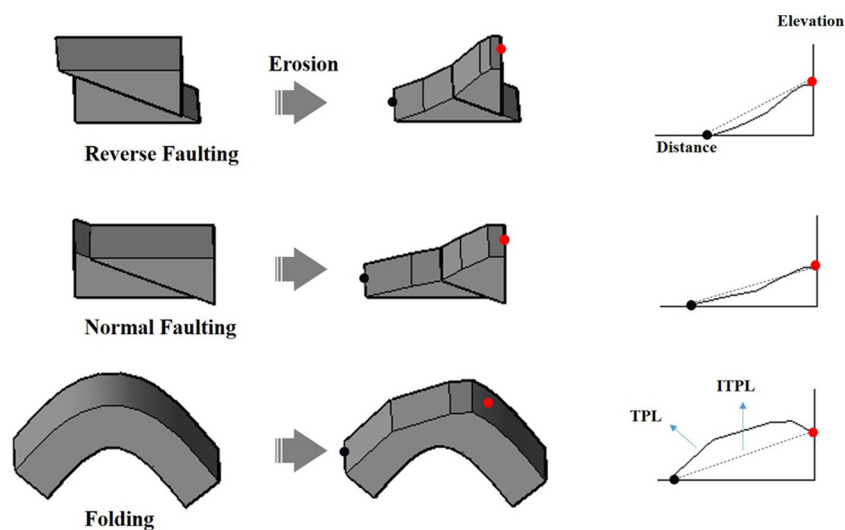


Fig. 8. A simple explanation of the general pattern of TPL and ITPL relative to each other in major tectonic activities including faulting and folding. The straight dashed lines show the ITPL from the starting to the ending point of hiking, and continuous lines show the TPL. The solid black and red circles represent the starting and ending points of hiking along a profile line, respectively

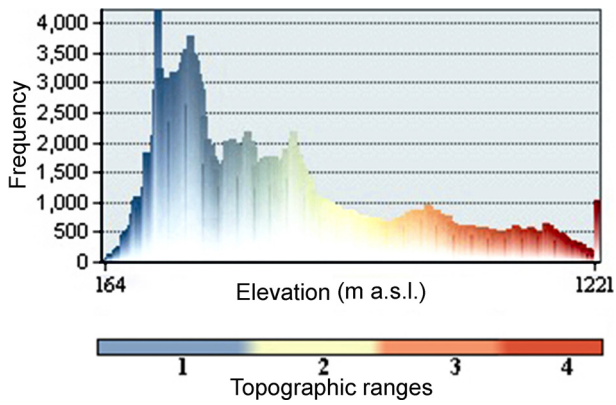


Fig. 9. An altitude histogram of sections shown in Figure 7, representing four topographic areas based on the frequency of elevation points

Topographic Slope Positions

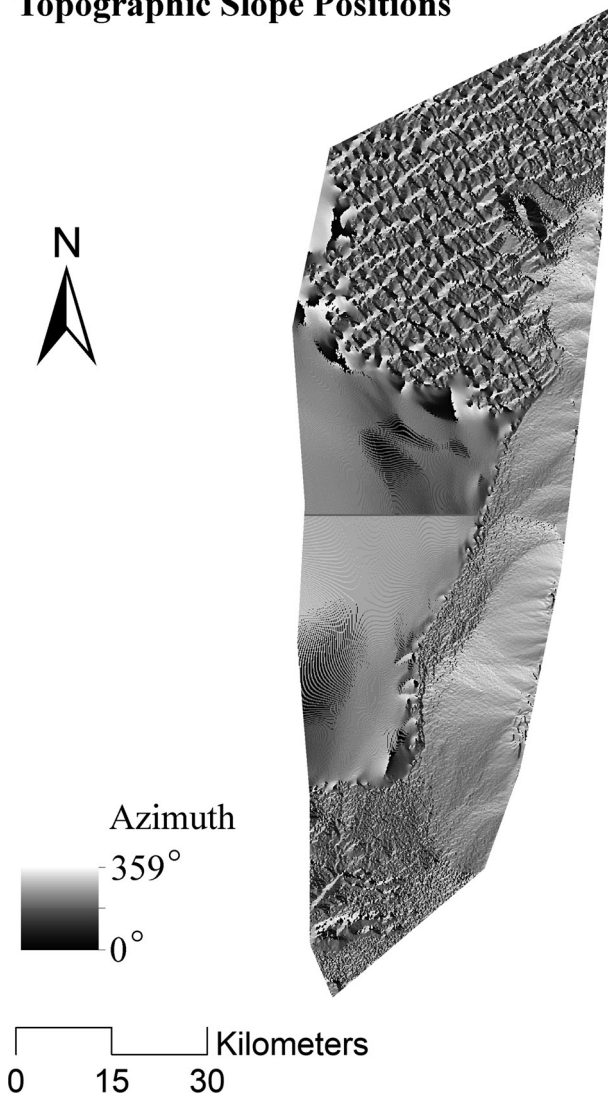


Fig. 10. Topographic Slope Position (TSP) map of the study area

points in the study area. A topographic slope position (TSP) map has also been created using equations 2 and 4 for the study area (Fig. 10). In addition, TSPC analysis within topographic regions separated from Figure 9 has been performed by histograms showing the frequency of slope classes (Fig. 11).

Among the topographic types, types A and C have been presented as the two main topographies with the highest correlation. Types B and D have also been introduced as two separate and sub-topographies with lesser correlation than the two types mentioned above.

In view of the fact that in the present study only the two items of continuity and slope have been analysed, the given score will be part of the final score of the index, and this is an example of scoring based on computational criteria.

The TCP graphs with the highest percentage of continuity associated with tectonic activities (50%) on the one hand and the lowest percentage of other continuities (20%) required for sufficient varia-

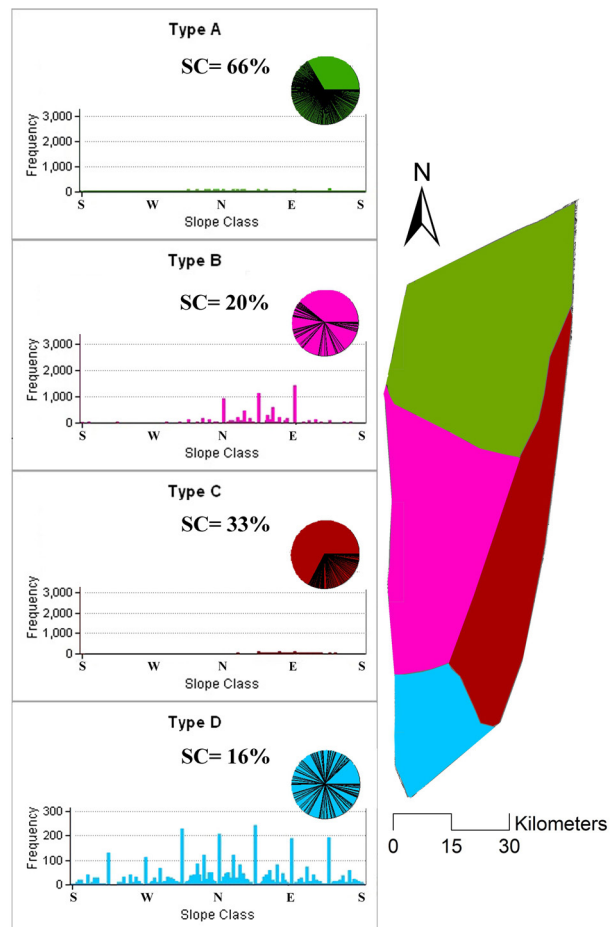


Fig. 11. TSPC analysis to classify slope correlation between topographic areas separated based on Figure 9. SC = Slope Correlation (in percent)

Table 1. Standard geodiversity scoring for continuity patterns in the study area

TCP	Percentage (%) ^a	Z – Sc	T – Sc	Sci _{sc}	C – NSci _{sc} ^b	Mean	STdev _p	ST _{sc}
SC	20.00	-1.07	39.31					
QC	50.00	1.34	63.36	0.92	0.74	33.33	12.47	150.00
CRC	30.00	-0.27	47.33					

^aTCP percentage is based on the number of sections containing particular pattern.

^bNormalized scientific score for TCP.

Table 2. Standard geodiversity scoring for slope positions in the study area

Region	TSPC (%) ^a	Z – Sc	T – Sc	Sci _{sc}	C – NSci _{sc} ^b	Mean	STdev _p	ST _{sc}
A	50.00	1.34	63.36					
B	20.00	-1.07	39.31					
C	33.00	-0.03	49.73	0.93	0.72	29.75	13.27	188.51
D	16.00	-1.39	36.10					

^aTSPC percentage is based on the ratio of slope classes to the number of slope positions in each region

^bNormalized scientific score for TSPC

tion in training purposes on the other, show that the geomorphological diversity of the study area is descriptively appropriate. However, statistically, it is necessary to score on the basis of equations 5 to 8 and the statistical parameters required for TCP analysis (Table 1). According to the calculated results for (, a score of 0.74 (out of 1) is suggested for the TCP item in the southeast Lut desert. In addition, the results of the TSPC analysis illustrate four types of topography in a single geomorphosite. Types A and C with the highest frequency correlations in slope position have been introduced as the two main TSPC types. Therefore, the existence of two main topographic types that cover most of the area, along with the other two sub-types B and D, indicate that the topographical diversity of the study area is descriptively appropriate. However, statistically, it is necessary to score on the basis of equations 5 to 8 and the statistical parameters required for TSPC analysis (Table 2). According to the calculated results for , a score of 0.72 (out of 1) is suggested for the TSPC item in the southeast Lut desert. In total, a score of 1.46 for both TCP and TSPC items which are part of the dv-index final score, has been included in the present study.

5. Conclusions

While scoring on all indices of geotouristic potential assessment, including scientific indices in the different models is done tastefully and descriptively, the present study demonstrates how scoring can be based on computable methods. Both scores related to TCP and TSPC analyses are part of the final score of the dv-index. The topographic area of the southeast Lut desert contains three patterns of SC, QC

and CRC continuities with a frequency of 20%, 50% and 30%, respectively. The high percentage of QC continuity represents the value of morphotectonic studies of the area alongside a suitable topography for visiting geotourists as a result of the presence of any topographic structural controllers, including folding and faulting along the eastern boundary of the study area. An overall score of 1.46 (out of 2) for both TCP and TSPC items confirms the sufficient geodiversity of topographic variations for educational purposes. Given the new approach of numerical computation in estimating scientific indices, the proposed methods need to be completed. It is suggested that other items of the dv-index, including geometrical patterns, genesis, geomorphic origin and structural elements of the geomorphs be considered for calculation of the final score.

Acknowledgements

We thank M. Salehi, A. Peyman and T. Rostami for sharing information and knowledge about the geology and access routes around the southeastern Lut desert.

References

- Adeyemi, T.O., 2011. The effective use of standard scores for research in educational management. *Research Journal of Mathematics and Statistics* 3, 91-96.
- Agard, P., Omrani, J., Jolivet, L. & Mouthereau, F., 2005. Convergence history across Zagros (Iran): constraints from collisional and earlier deformation. *International Journal of Earth Sciences* 94, 401-419.
- Alexander, J. & Leeder, M.R., 1987. Active tectonic control on alluvial architecture. [In:] F.G. Ethridge, R.M.

- Flores & M.D. Harvey (Eds): *Recent Development in Fluvial Sedimentology*. SEPM, Tulsa, Special Publication, 39, 243–252.
- Berberian, M., 1995. Master “blind” thrust faults hidden under the Zagros folds: active basement tectonics and surface morphotectonics. *Tectonophysics* 241, 193–224.
- Buckley, R., 2003. Environmental inputs and outputs in ecotourism: Geotourism with a positive triple bottom line? *Journal of Ecotourism* 2, 76–82.
- Burlando, M., Firpo, M., Queirolo, C., Rovere, A. & Vacchi, M., 2011. From geoheritage to sustainable development: strategies and perspectives in the Beigua Geopark (Italy). *Geoheritage* 3, 63–72.
- Comanescu, L., Nedelea, A. & Dobre, R., 2012. The Evaluation of Geomorphosites from the Ponoare Protected Area. *Forum Geografici Studii și Cercetări de Geografie și Protecția Mediului* 11, 54–61.
- Coratza, P. & Giusti, C., 2005. Methodological proposal for the assessment of the scientific quality of geomorphosites. *Il Quaternario* 18, 307–313.
- Corbi, H., Fierro, L., Aberasturi, A. & Ferris, E.J.S., 2018. Potential use of a significant scientific geosite: the Messinian coral reef of Santa Pola (SE Spain). *Geoheritage* 10, 427–441.
- Dowling, R. & Newsome, D., 2006. Geotourism’s issues and challenges. *Geotourism* 242–254.
- Drewes, H., 1972. *Geological Survey Professional Paper* 717–719. U.S. Government Printing Office, California, 350 pp.
- Ehsani, A.H. & Quiel, F., 2008. Application of self organizing map and SRTM data to characterize yardangs in the Lut desert, Iran. *Remote Sensing of Environment* 112, 3284–3294.
- Farbod, Y., Bellier, O., Shabani, E. & Abbassi, M.R., 2011. Geomorphic and structural variations along the Doruneh Fault System (central Iran). *Tectonics* 30, TC6014.
- Farsani, N.T., Coelho, C.O. & Costa, C., 2013. Rural geotourism: A new tourism product. *Acta Geoturistica* 4, 1–10.
- Ferrer-Valero, N., 2018. Measuring geomorphological diversity on coastal environments: A new approach to geodiversity. *Geomorphology* 318, 217–229.
- Forte, J.P., Brilha, J., Pereira, D.I. & Nolasco, M., 2018. Kernel density applied to the quantitative assessment of geodiversity. *Geoheritage* 10, 205–217.
- Ghods, M., 2017. Morphometric characteristics of Yardangs in the Lut Desert, Iran. *Desert* 22, 21–29.
- Habibi, T., Golubova, N.V. & Ruban, D.A., 2017. New evidence of highly-complex geological heritage in Iran: Miocene sections in the Zagros Fold-Thrust Belt. *GeoResJ* 13, 96–102.
- Hadžić, O., Marković, S.B., Vasiljević, D.A. & Nedeljković, M., 2010. A Dynamical Model for Assessing Tourism Market Attractiveness of a Geosite. *1st International Conference on Geoheritage & Geotourism Research GEOTRENDS 2010*, Novi Sad. Abstract book, 23–27.
- Horváth, G. & Csüllög, G., 2012. The role of ecotourism and Geoheritage in the spatial development of former mining regions. [In:] P. Wirth, MB. Cernic & W. Fischer (Eds): *Post-mining regions in Central Europe, Problems, Potentials, Possibilities*. Oekom Verlag, Muenchen, 226–240.
- Hose, T.A., 2012. 3G’s for modern geotourism. *Geoheritage* 4, 7–24.
- Hosseinzadeh, M.M., Khaleghi, S., Maromi, H.Z. & Sadough, S.H., 2018. Geomorphosite assesment in Qeshm Geopark (Iran). *Turizam: Medunarodni znanstveno-stručni časopis* 66, 428–442.
- Hurtado, H., Dowling, R. & Sanders, D., 2014. An exploratory study to develop a geotourism typology model. *International Journal of Tourism Research* 16, 608–613.
- Jana, J., Matúš, J. & Gejza, M.T., 2016. Social tourism, its clients and perspectives. *Mediterranean Journal of Social Sciences* 7, 42–52.
- Kreyszig, E., 1979. *Applied Mathematics*. Wiley Press, New York, 880 pp.
- Kubalíková, L., Kirchner, K., & Bajer, A., 2017. Secondary geodiversity and its potential for urban geotourism: a case study from Brno city, Czech Republic. *Quaestiones Geographicae* 36, 63–73.
- Maghsoudi, M. & Emadoldin, S., 2007. Evaluation of geotourism properties of the Lut desert landforms. *Tourism Management Studies* 6, 95–108 (in Persian).
- Maghsoudi, M., Hajizadeh, A., Nezammahalleh, M.A. & Bayati Sedaghat, Z., 2017. New method for measurement of barchans parameters Case study: Lut desert, Iran. *Desert* 22, 11–19.
- Mehdipour Ghazi, J., Ólafsdóttir, R., Tongkul, F. & Mehdipour Ghazi, J., 2013. Geological features for geotourism in the western part of Sahand Volcano, NW Iran. *Geoheritage* 5, 23–34.
- Melelli, L., 2019. Geotourism through multimedia exhibition: improving the access to Urban Geoheritage. *Resources* 8, 148.
- Melelli, L., Vergari, F., Liucci, L. & Del Monte, M., 2017. Geomorphodiversity index: Quantifying the diversity of landforms and physical landscape. *Science of the Total Environment* 584, 701–714.
- Mikhailenko, A.V., & Ruban, D.A., 2019. Geo-heritage specific visibility as an important parameter in geo-tourism resource evaluation. *Geosciences* 9, 146.
- Moghimi, E., 2009. comparative study of changing drainage basin system with tectonic forms, case study: Lut block, Iran. *American Journal of Applied Sciences* 6, 1270.
- Nemanj, T., 2011. The potential of Lazar Canyon (Serbia) as a geotourism destination: Inventory and evaluation. *Geographica Pannonica* 15, 103–112.
- Neukrug, E.S. & Fawcett, R.C., 2014. *Essentials of testing and assessment: A practical guide for counselors, social workers, and psychologists*. Cengage Learning, Mason, 368 pp.
- Oliver, T. & Jenkins, T., 2003. Sustaining rural landscapes: The role of integrated tourism. *Landscape Research* 28, 293–307.
- Panizza, M., 2001. Geomorphosites: Concepts, methods and examples of geomorphological survey. *Chinese Science Bulletin* 46, 4–5.
- Patro, S. & Sahu, K.K., 2015. Normalization: A preprocessing stage. *International Advanced Research Journal in Science, Engineering and Technology* 2, 20–22.

- Pereira, D., Brilha, J. & Dias, G., 2008. Master's course on Geological Heritage and Geoconservation. *European Geologist* 26, 29–31.
- Pica, A., Vergari, F., Fredi, P. & Del Monte, M., 2016. The Aeterna Urbs geomorphological heritage (Rome, Italy). *Geoheritage* 8, 31–42.
- Reynard, E. & Brilha, J., 2017. *Geoheritage: assessment, protection, and management*. Elsevier, Amsterdam, 482 pp.
- Reynard, E. & Panizza, M., 2005. Geomorphosites: definition, assessment and mapping. An introduction. *Géomorphologie: Relief, Processes, Environnement* 11, 177–180.
- Reynard, E., Pica, A. & Coratza, P., 2017. Urban geomorphological heritage. An overview. *Quaestiones Geographicae* 36, 7–20.
- Rocha, F. & da Silva, E.F., 2014. Geotourism, medical geology and local development: Cape Verde case study. *Journal of African Earth Sciences* 99, 735–742.
- Rodrigues, M.L., Machado, C.R. & Freire, E., 2011. Geotourism routes in urban areas: a preliminary approach to the Lisbon geoheritage survey. *GeoJournal of Tourism and Geosites* 8, 281–294.
- Salvia, J., Ysseldyke, J. & Witmer, S., 2012. Assessment: In special and inclusive education. Cengage Learning, Mason, 432 pp.
- Scheyvens, R., 1999. Ecotourism and the empowerment of local communities. *Tourism Management* 20, 245–249.
- Stocklin, J., 1968. Structural history and tectonics of Iran: a review. *AAPG Bulletin* 52, 1229–1258.
- Stoffelen, A. & Vanneste, D., 2015. An integrative geotourism approach: Bridging conflicts in tourism landscape research. *Tourism Geographies* 17, 544–560.
- Suzuki, D.A. & Takagi, H., 2018. Evaluation of geosite for sustainable planning and management in geotourism. *Geoheritage* 10, 123–135.
- Taherpour Khalil Abad, M., Valipour, F., Ibrahim, M., Torshizian, H.A., Taherpour Khalil Abad, V. & Asmaryan, S., 2012. The geotourism potential investigations in Kashmar Area, Khorasan-e-Razavi Province, NE Iran. *Iranian Journal of Earth Sciences* 4, 51–60.
- Vico, G. & Porporato, A., 2009. Probabilistic description of topographic slope and aspect. *Journal of Geophysical Research: Earth Surface* 114(F1).
- Vincent, S.J., Allen, M.B., Ismail-Zadeh, A.D., Flecker, R., Foland, K.A., & Simmons, M.D., 2005. Insights from the Talysh of Azerbaijan into the Paleogene evolution of the South Caspian region. *Geological Society of America Bulletin* 117, 1513–1533.
- Walker, R.T., Gans, P., Allen, M. B., Jackson, J., Khatib, M., Marsh, N. & Zarrinkoub, M., 2009. Late Cenozoic volcanism and rates of active faulting in eastern Iran. *Geophysical Journal International* 177, 783–805.
- Wimberley, R.C., 1975. A program for the T-score normal standardizing transformation. *Educational and Psychological Measurement* 35, 693–695.
- Zwoliński, Z., Najwer, A. & Giardino, M., 2018. Methods for assessing geodiversity. [In:] *Geoheritage*, Elsevier, pp. 27–52.

Manuscript received 20 June 2019
Revision accepted 15 February 2020